

Review Article

Synthesis and Application of One-Dimensional $\text{La}(\text{OH})_3$ Nanostructures: An Overview

Xiang Xiao,¹ Yu Huang,² and Fan Dong¹

¹Chongqing Key Laboratory of Catalysis and Functional Organic Molecules, College of Environmental and Biological Engineering, Chongqing Technology and Business University, Chongqing 400067, China

²Key Laboratory of Aerosol Science & Technology, SKLLQG, Institute of Earth Environment, Chinese Academy of Sciences, Xi'an 710075, China

Correspondence should be addressed to Fan Dong; dfctbu@126.com

Received 19 June 2014; Accepted 1 August 2014; Published 21 August 2014

Academic Editor: Yu Xin Zhang

Copyright © 2014 Xiang Xiao et al. This is an open access article distributed under the Creative Commons Attribution License, which permits unrestricted use, distribution, and reproduction in any medium, provided the original work is properly cited.

One-dimensional (1D) semiconductor nanomaterials are of particular importance owing to their unique properties and potential applications. This review attempts to provide a comprehensive introduction of 1D $\text{La}(\text{OH})_3$ nanostructures including nanowires, nanoneedles, nanobelts, and nanorods. Firstly, various strategies developed to fabricate the 1D $\text{La}(\text{OH})_3$ nanostructures are discussed, such as precipitation and composite-hydroxide-mediated, hydrothermal, and solvothermal methods, accompanying the description of the corresponding growth mechanisms. Then, the unique properties such as novel physical properties of 1D $\text{La}(\text{OH})_3$ nanostructures resulting from their unique electronic structures and numerous transition modes involving the 4f shells of these ions are represented in detail. Also, the wide applications in photocatalyst, capacitors, and photoluminescence based on the unique properties are discussed. Finally, the paper ends with a summary and some perspectives on the challenges and new directions in this emerging area.

1. Introduction

The properties of nanosized materials strongly depend on their size, shape, and morphology [1, 2]. Recently, one-dimensional (1D) nanostructures have attracted great attention due to their unique physical, chemical, and mechanical properties. Moreover, their particular optical, electrical, and thermal properties result in the wide applications, while solution phase synthesis of controlled one-dimensional (1D) nanostructures such as nanowires, nanobelts, nanorods, and nanotubes is still a challenging task as surface energy favours the spherical particle formation [3]. Thus, much effort has been devoted to fabricate 1D nanostructures by either deploying surfactants/polymer as capping agent or using templates. Up till now, several strategies have been developed to prepare 1D nanostructure materials, such as electrochemical methods, precipitation method, template directed growth technique, vapor-liquid-solid (VLS) synthesis, composite-hydroxide-mediated (CHM) method, and hydrothermal process.

Generally speaking, lanthanide compounds with 1D nanostructure promise as highly functionalized materials as a result of their specific shapes and quantum size effects. Also, as a consequence of their unique electronic structures and exhibiting numerous transition modes involving the 4f shells of their ions, lanthanum and its compounds have the outstanding optical, electrical, and magnetic properties [4–7]. Lanthanum, the lightest element in the lanthanide series, has been widely studied in its oxide, hydroxide, and phosphate forms and has been extensively applied in optoelectronic devices, catalysis, sensors, sorbent, solid electrolyte, and so forth. Particularly, the study of one-dimensional $\text{La}(\text{OH})_3$ has attracted growing interest because of the promising applications in lanthanum hydroxide nanowires modified carbon paste electrode (LNW/CPE), catalyst, sorbent materials, sensors, and the process for the collection of As(III).

Various chemical methods are adopted for the preparation of lanthanum hydroxide nanostructures, including solvothermal, hydrothermal, and CHM methods. For example, Wang et al. [8, 9] reported the synthesis of $\text{La}(\text{OH})_3$

nanorods and nanotubes through a hydrothermal method. Hu et al. [10] synthesized $\text{La}(\text{OH})_3$ nanobelts through a CHM method and then transformed to La_2O_3 nanobelts via further calcinations. $\text{La}(\text{OH})_3$ nanorods with controlled morphology were also prepared by a nonaqueous method [11]. In addition, Wang and Li [12] reported a simple method for large-scale synthesis of $\text{La}(\text{OH})_3$ nanowires.

Herein, this paper will provide a comprehensive review of the state-of-the-art research activities that focus on the synthetic strategies and applications of one-dimensional $\text{La}(\text{OH})_3$. This review is divided into two main sections. The first section introduces the synthetic methods of $\text{La}(\text{OH})_3$. These approaches are classified into precipitation, CHM, and solvothermal and hydrothermal methods. Besides, this section also discusses influence factors during the preparation process: the pH value, temperature, alkaline sources, and surfactant, and the use of microwaves assisted in the hydrothermal treatment. It can be found that these factors play a crucial role in controlling the morphologies of the products. Based on these fundamental physical properties of $\text{La}(\text{OH})_3$, the recent progress of their application will be highlighted in the next section, which includes photocatalyst, photoluminescence, and fabrication of capacitors. This paper will conclude with a prospective outlook of some scientific and technological challenges with respect to further investigation in this field.

2. Synthesis of One-Dimensional $\text{La}(\text{OH})_3$ Nanostructures

A variety of methods have been utilized to synthesize 1D $\text{La}(\text{OH})_3$ nanostructures. According to the synthesis environment, they can be mainly divided into four categories: precipitation, CHM, hydrothermal, and solvothermal methods. This section will present a survey of various reports on the synthesis of 1D $\text{La}(\text{OH})_3$ nanostructures using these methods.

2.1. Precipitation Method. The precipitation method is widely adopted because of its simplicity, high efficiency, and low cost. According to the precipitation method, a base ($\text{NH}_3\cdot\text{H}_2\text{O}$, NaOH , KOH) was added into a La^{3+} -contained solution under magnetic stirring and reacted sufficiently for certain time. Several precipitation approaches have been developed to synthesize one-dimensional $\text{La}(\text{OH})_3$ nanostructure.

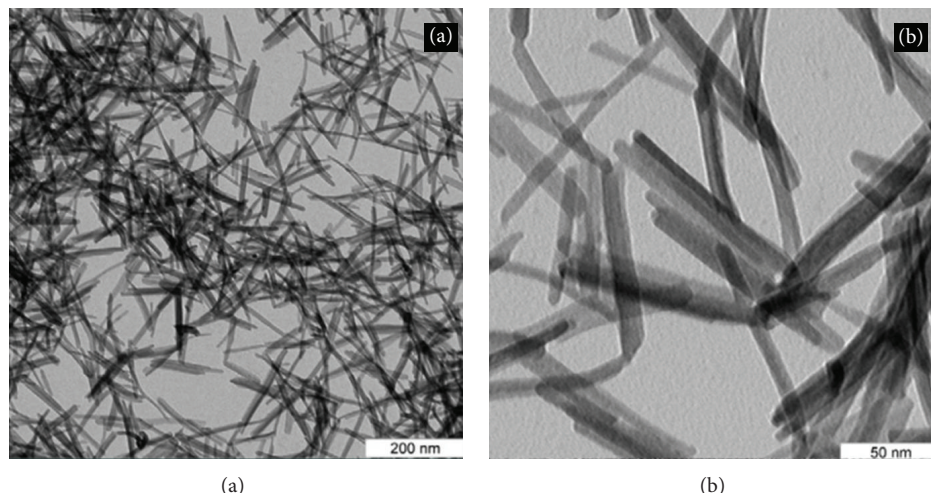
Mu et al. [13] have obtained $\text{La}(\text{OH})_3$ nanorods with uniform morphology with aspect ratio of about 10–15. The TEM images of Figure 1 illustrate the obtained samples exhibited one-dimensional rod-like nanostructures. With the concentration of CTAB increasing from 0.002 to 0.006 M, the length and radius of the $\text{La}(\text{OH})_3$ nanorods also increased. The cationic surfactant CTAB not only provides a favorable site for the growth of the particulate assemblies, but also influences the formation process, including nucleation, growth, coagulation, and flocculation [14]. While Li et al. [15] added diethylenetriamine to induce the centripetal growth of $\text{La}(\text{OH})_3$ nanostructures, which acts not only as an alkaline source, but also as a surfactant. A possible growth process of dendrite-like $\text{La}(\text{OH})_3$ nanostructures can be described

as follows. The OH^- is slowly released and reacts with La^{3+} , and the resulting $\text{La}(\text{OH})_3$ nucleates and aggregates in the presence of diethylenetriamine. The anisotropic growth and Ostwald aging lead to the dendrite-like nanostructures, while only nanorods can be achieved using sodium hydroxide and ammonia as mineralizer instead of diethylenetriamine, which confirmed the importance of diethylenetriamine as a surfactant.

Kohli et al. [16] synthesized $\text{La}(\text{OH})_3$ nanorods with length varying from 30 to 50 nm with aspect ratio of 2–5 in aqueous solution using hydrazine hydrate as alkaline sources and using cationic CTAB and TBAB as surfactants. Lanthanum ions quickly react with hydroxyl ions to form lanthanum hydroxide because of electrostatic interactions. Due to the cationic group of surfactants molecules present in the reaction mixture, the coordinate complex $\text{La}(\text{OH})_4^{-1}$ occurs. Thus cation CTA^+ got adsorbed on the surface of $\text{La}(\text{OH})_4^{-1}$ to form a film. The film acts as seeding source for the assembly and growth of nanocrystal in the form of rods. The surfactant serves as a growth controller as well as agglomeration inhibitor by forming a covering film on the $\text{La}(\text{OH})_3$ rods. Adding CTAB alone in the reaction mixture resulted in formation of long fibres, while short size anisotropic rods were obtained in the presence of both CTAB and TBAB mixture due to the fact that TBAB can restrict the faster longitudinal growth to some extent.

Figure 1 is reproduced from the report of Mu et al. [13]. From Figure 1, we can find that the as-prepared $\text{La}(\text{OH})_3$ samples exhibited one-dimensional rod-like nanostructures with hexagonal phase. Moreover, the $\text{La}(\text{OH})_3$ nanostructures are monodisperse and display uniform size and shape with 13–15 nm in width and 150–200 nm in length (CTAB concentration is 0.004 M).

2.2. Composite-Hydroxide-Mediated Method. Composite-hydroxide-mediated (CHM) synthesis method [21, 22] can not only synthesize complex oxide nanostructures, but also produce hydroxide nanostructures under normal atmospheric pressure. Hu et al. [10] have developed a facile CHM synthesis method to prepare ultralong $\text{La}(\text{OH})_3$ nanobelts. The associated SEM images were shown in Figure 2. Lanthanum hydroxide nanobelts were prepared by adding 0.1 g $\text{La}(\text{CH}_3\text{COO})_3$ to a mixture of hydroxides ($\text{NaOH}/\text{KOH} = 51.5 : 48.5$) in a Teflon vessel and treated at 200°C for 48 h in a furnace. The $\text{La}(\text{OH})_3$ nanobelts are single-crystalline with a [110] growth direction. The possible growth mechanism for the $\text{La}(\text{OH})_3$ nanobelts is as follows. In the molten hydroxide, $\text{La}(\text{CH}_3\text{COO})_3$ reacts with NaOH/KOH to produce crystalline $\text{La}(\text{OH})_3$ nuclei, which then grow along the [110] direction to form nanobelts. In this growth mechanism, disperse single-crystalline nanostructures can also be obtained in the absence of any surface-capping materials. The large viscosity of the hydroxide led to low growth rates, resulting in slow formation of $\text{La}(\text{OH})_3$ nanostructures. Moreover, the melting points (T_m) of both pure sodium hydroxide and potassium hydroxide are over 300°C, and the eutectic point for the composition $\text{NaOH}/\text{KOH} = 51.5 : 48.5$ is only about 165°C. Therefore, during the reaction process,

FIGURE 1: The typical TEM images of the $\text{La}(\text{OH})_3$ nanorods [13].TABLE 1: Summary of preparation process of $\text{La}(\text{OH})_3$ nanostructure by precipitation.

Reference	Preparation method	Morphology	Mechanism of formation
[13]	<ol style="list-style-type: none"> ① 0.004 M CTAB was mixed with distilled deionized water. ② Then 10 mL $\text{NH}_3 \cdot \text{H}_2\text{O}$ was added into the CTAB solution. ③ 0.04 M $\text{LaCl}_3 \cdot 7\text{H}_2\text{O}$ was added into it and stirred for 2 h. 	Nanorods	$\text{La}^{3+} + 3\text{OH}^- \rightarrow \text{La}(\text{OH})_3$.
[15]	<ol style="list-style-type: none"> ① $\text{La}(\text{NO}_3)_3$ was dissolved (solution A). ② Diethylenetriamine was dissolved (solution B). ③ The solution A was heated at 90°C and solution B was dropped into solution A and then kept for 3 h. 	Dendrite-like $\text{La}(\text{OH})_3$ nanostructures	$\text{La}^{3+} + 3\text{OH}^- \rightarrow \text{La}(\text{OH})_3$.
[16]	<ol style="list-style-type: none"> ① 5 mM of each CTAB, TBAB, and $\text{La}(\text{NO}_3)_3 \cdot 6\text{H}_2\text{O}$ was dissolved. ② 1.215 mL of hydrazine hydrate was added rapidly to this reaction mixture. 	Nanorods	$\text{N}_2\text{H}_4 + \text{H}_2\text{O} \leftrightarrow \text{N}_2\text{H}_5^+ + \text{OH}^-$ $\text{La}^{3+} + \text{OH}^- \rightarrow \text{La}(\text{OH})_3$

the hydroxides not only act as reactants, but also play a role as solvents for lowering the reaction temperature. The summary of preparation process for $\text{La}(\text{OH})_3$ nanostructures by precipitation is shown in Table 1.

2.3. Hydrothermal Method. Hydrothermal process began with aqueous mixture of soluble metal salt of the precursor materials. Usually the mixed solution is placed in an autoclave under elevated temperature and relatively high pressure conditions. Many works have been reported to systematically manipulate uniform morphologies and well-dispersed 1D $\text{La}(\text{OH})_3$ materials using hydrothermal approaches. In addition, according to the different heating methods, the hydrothermal method is divided into two categories: conventional hydrothermal and microwave-assisted hydrothermal methods.

2.3.1. Conventional Hydrothermal Method. In the traditional hydrothermal method, lanthanum hydroxide gel was firstly synthesized by precipitation or by the direct mixture of a lanthanum salt with a base solution and then transferred to Teflon autoclave and heated at an oven. Jia et al. [17] have reported that the morphologies of $\text{La}(\text{OH})_3$ can be modulated by adjusting the pH values of the initial solution. A higher pH value implies a higher OH^- concentration and a higher

chemical potential in solution. Therefore, the nucleating process occurs faster and more nuclei of crystals are formed, resulting in the high aspect ratio of the samples. In addition, the field SEM images of Figure 3 illustrated that alkaline sources exerted significant effect on the preferential growth orientations. While using hydrazine hydrate ($\text{N}_2\text{H}_4 \cdot \text{H}_2\text{O}$) as alkaline source, $\text{La}(\text{OH})_3$ nanoprisms will be obtained. The aspect ratio of the $\text{La}(\text{OH})_3$ nanoprisms reduces with an increase in the concentration of $\text{N}_2\text{H}_4 \cdot \text{H}_2\text{O}$. The hydrazine hydrate may have dual functions in the formation process of $\text{La}(\text{OH})_3$, acting as alkaline sources in the solution and behaving as crystal facet inhibitors in the system.

Wang et al. [18] have synthesized stable and crystalline phase Ln (Ln = Sm, Er, Gd, Dy, and Eu) doped $\text{La}(\text{OH})_3$ ($\text{La}(\text{OH})_3 : \text{Ln}^{3+}$) nanorods. The as-prepared $\text{La}(\text{OH})_3 : \text{Ln}^{3+}$ samples are one-dimensional rod-like nanostructures, and the $\text{La}(\text{OH})_3 : \text{Ln}^{3+}$ products with 20% Ln^{3+} doped are mainly composed of uniform short nanorods with diameters of about 10 nm and lengths of 100–150 nm. The Ln doping does not change the hexagonal structure of $\text{La}(\text{OH})_3$, which implies that the Ln^{3+} doping most probably occurs by substituting lanthanum atom in the crystal structure. Similarly, Zhang et al. [20] have prepared uniform $\text{Yb}^{3+}/\text{Er}^{3+}$, $\text{Yb}^{3+}/\text{Ho}^{3+}$, and $\text{Yb}^{3+}/\text{Tm}^{3+}$ codoped $\text{La}(\text{OH})_3$ microrods in molten composite-hydroxide (NaOH/KOH) medium, while

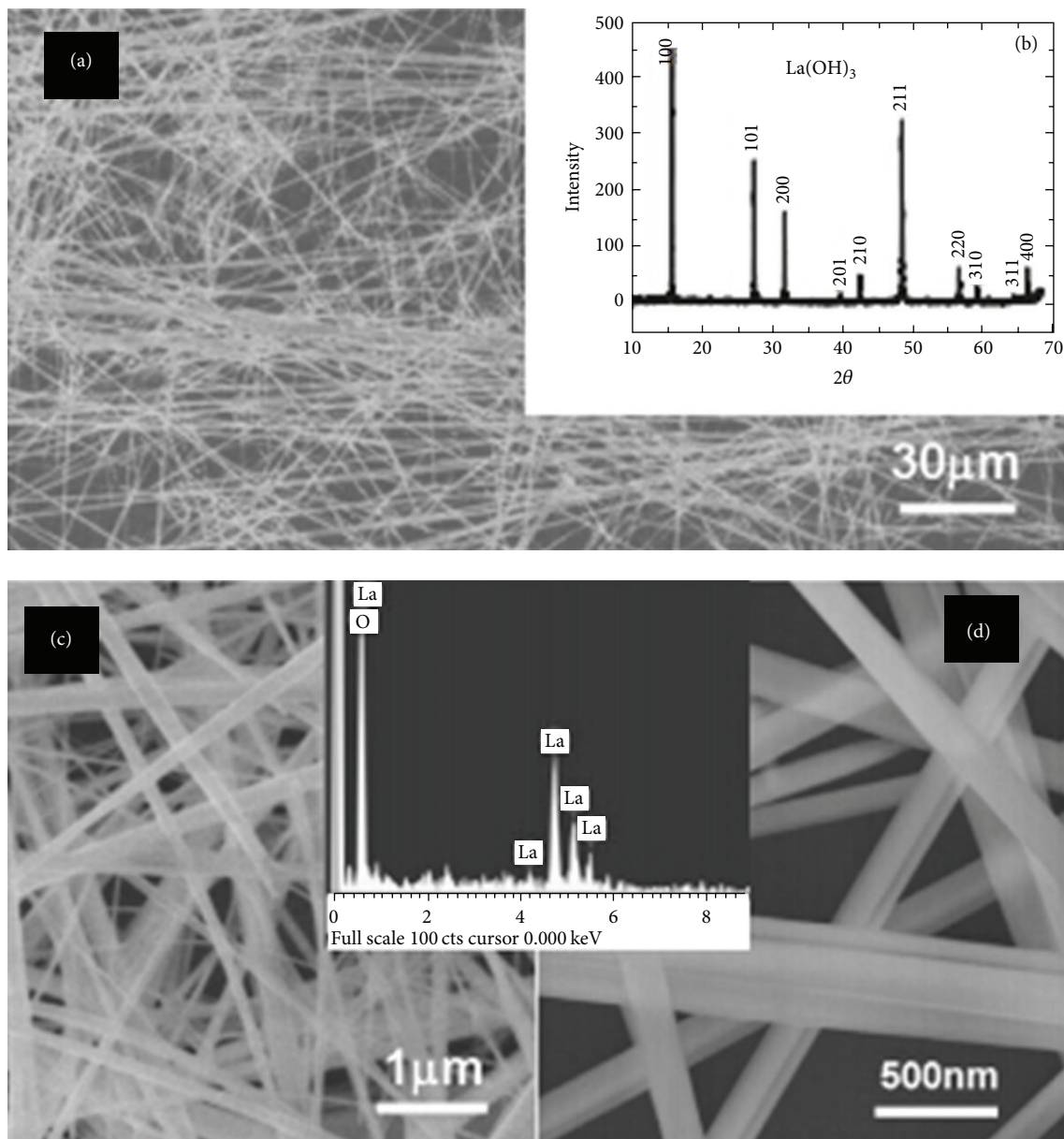


FIGURE 2: (a) Low-magnification SEM image of the $\text{La}(\text{OH})_3$ products. (b) A typical XRD pattern of the as-synthesized $\text{La}(\text{OH})_3$ product. (c) and (d) are the high-magnification SEM images of the $\text{La}(\text{OH})_3$ product [10].

the $\text{La}_2\text{O}_3 : \text{Ln}^{3+}$ ($\text{Ln} = \text{Yb}/\text{Er}, \text{Yb}/\text{Tm}, \text{Yb}/\text{Ho}$) microrods were obtained by solid state reaction at 700°C for 6 h. In the synthesis, no catalyst, template, or surfactant were used in the reaction system to reduce the surface energy, so the growth of $\text{La}(\text{OH})_3 : \text{Ln}^{3+}$ is governed by the inherent crystal structure and the chemical activity. The growth mechanism of microrods formation is proposed as follows. After the hydroxides are molten, La^{3+} cations can easily react with hydroxyl groups to form $\text{La}(\text{OH})_3$ nuclear due to the opposite electric charge, whereas a large number of Ln^{3+} and OH^- ions still exist in the solution, which will be adsorbed on the preferred surfaces of $\text{La}(\text{OH})_3$ nuclear. Therefore, long $\text{La}(\text{OH})_3 : \text{Ln}^{3+}$ microrods will form with the increasing

reaction time. $\text{La}_2\text{O}_3 : \text{Ln}^{3+}$ microrods can be topochemically prepared from $\text{La}(\text{OH})_3 : \text{Ln}^{3+}$ after the thermal decomposition process [23].

2.3.2. Microwave-Assisted Hydrothermal Method. In the micro-wave process, heat is internally generated within the material, instead of originating from external heating sources [24]. Microwave radiation as a heating source is applied for the hydrothermal method, which is beneficial to improve the reaction kinetic constants [25]. Additionally, microwave-assisted hydrothermal method has several advantages compared to the conventional hydrothermal: less energy

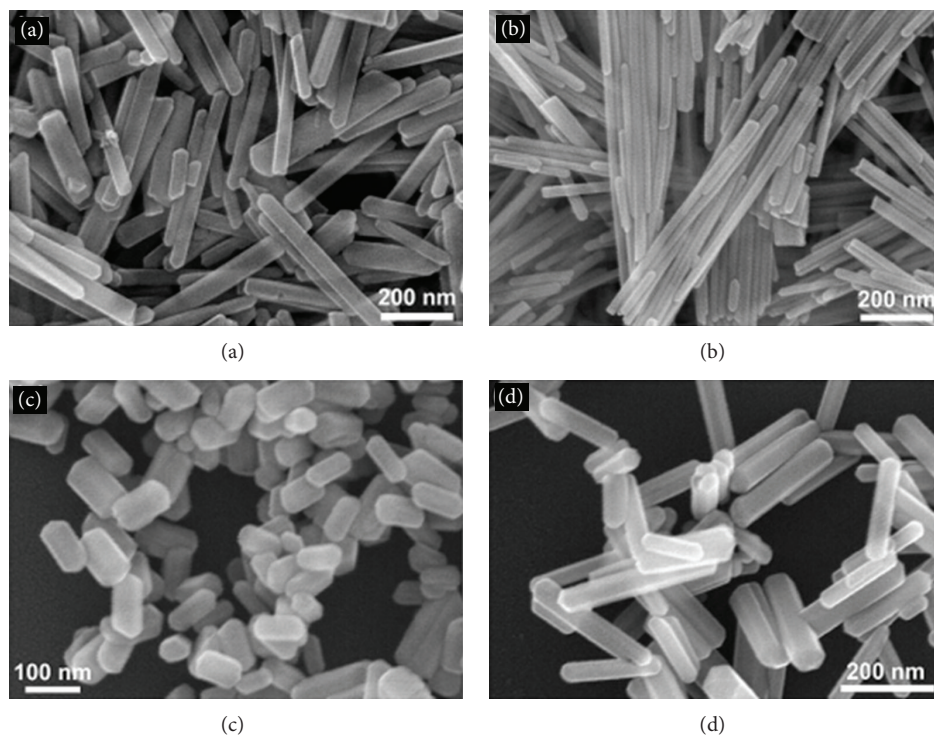


FIGURE 3: The SEM images of the $\text{La}(\text{OH})_3$ samples prepared at (a) pH = 7 and (b) pH = 10 with ammonia as alkaline source and (c) at pH = 9 with pure hydrazine hydrate and (d) a mixture of ammonia and hydrazine hydrate as alkaline sources [17].

consumption, shorter reaction time, lower synthetic temperature, higher purity, and smaller particle size [26, 27]. Pao et al. [19] have reported that uniform $\text{La}(\text{OH})_3$ nanowires (NWs) with a high aspect ratio of more than 200 have been successfully synthesized by a simple microwave-assisted hydrothermal (MH) process. Compared to a conventional hydrothermal (CH) one, the $\text{La}(\text{OH})_3$ nanorods are obtained in a lower aspect ratio, higher temperature, and longer time. The formation mechanism of 1D $\text{La}(\text{OH})_3$ NWs synthesized by the MH method was explained by an ionic solvent effect [28]. Concentrated NH_4OH was added into a solution containing La^{3+} cations and the La^{3+} cations can react with OH^- anions to form $(\text{La}(\text{OH})_4)^-$. Then the positive NH_4^+ ions interact with $(\text{La}(\text{OH})_4)^-$ to form $\text{NH}_4\text{La}(\text{OH})_4$ gel complexes by the electrostatic interaction. On the optimal conditions, NH_4^+ and OH^- ions were released from $\text{NH}_4\text{La}(\text{OH})_4$, and $\text{La}(\text{OH})_3$ molecules nucleated and grew in the lowest energy plane at the highest growth rate as $\text{La}(\text{OH})_3$ NWs were produced.

Figure 3 is achieved from the report of Jia et al. [17]. The report indicated that the pH value of $\text{NH}_3\cdot\text{H}_2\text{O}$ as alkaline sources increased from 7 to 9, and the aspect ratio of the $\text{La}(\text{OH})_3$ nanowires increased dramatically [17]. By increasing the pH value to 10, the nanowires self-assembled into bundles along their cross-sectional diameter through a direct aggregation growth process. When hydrazine hydrate ($\text{N}_2\text{H}_4\cdot\text{H}_2\text{O}$) is applied as alkaline source, the as-prepared sample is almost entirely composed of short hexagonal nanoprisms. However, when the mixtures of ammonia and hydrazine hydrate are used as alkaline sources (pH 9), the

sample consisting of uniform hexagonal nanoprisms with higher aspect ratios was produced. The aspect ratios of the samples reduce with an increase in the concentration of $\text{N}_2\text{H}_4\cdot\text{H}_2\text{O}$.

2.4. Solvothermal Method. With the advantages of high purity and good homogeneity, the solvothermal synthesis method is one of the most significant technologies for the preparation of nanorods or nanowires [29]. The solvothermal process with low boiling point not only shortens reactant times, but also benefits the crystallinity of products [30]. Tang et al. [31] applied a sol-solvothermal method to synthesize $\text{La}(\text{OH})_3$ and used microwave radiation to dry the $\text{La}(\text{OH})_3$ nanorods. In this experiment, 60 mL 0.3 M $\text{NH}_3\cdot\text{H}_2\text{O}$ was added to 20 mL 0.1 M aqueous $\text{La}(\text{NO}_3)_3$ to get a light blue transparent sol. After the sol was washed with ethanol and dispersed into 16 mL benzene, the pH value was adjusted to 12 by adding n-butylamine. The products were dried for 4 min using a microwave oven. The obtained $\text{La}(\text{OH})_3$ nanorods are single crystals and uniform with diameters ranging from 8 to 15 nm and lengths of up to 200 nm. If conventional heating is applied, the morphology of $\text{La}(\text{OH})_3$ is irregular due to the aggregation of the nanostructures. Therefore, microwave radiation drying can keep their morphologies better than conventional drying. In contrast to conventional drying, microwave drying evaporation takes place on the surface of the sample at lower temperature because of evaporative cooling, which further ensures a more stable temperature-increasing process, effectively preventing the agglomeration

TABLE 2: Summary of preparation process of La(OH)₃ nanostructure by hydrothermal method.

Reference	Preparation method	Morphology	Mechanism of formation
[17]	① Ammonia solution was added to La(NO ₃) ₃ (1 M, 2 mL) aqueous solution. ② After additional agitation for 1 h, the as-obtained colloidal suspension was transferred to a 50 mL autoclave and heated at 200 °C for 24 h.	PH 7 to 9: nanowire. PH 10: nanobundles	$\text{La}^{3+} + \text{OH}^- \rightarrow \text{La(OH)}_3$
[18]	① 0.003 M CTAB was mixed with deionized water and then 40 mL of NH ₃ ·H ₂ O was added. ② 0.004 M LaCl ₃ ·6H ₂ O and LnCl ₃ ·6H ₂ O with the different Ln compositions were added into the mixture and then heated at 200 °C for 4 h.	Nanorods	$\text{La}^{3+} + \text{OH}^- \rightarrow \text{La(OH)}_3$
[19]	① La(NO ₃) ₃ , Yb(NO ₃) ₃ , and Er(NO ₃) ₃ and deionized water were added into a 30 mL Teflon-lined autoclave, followed by adding mixed hydroxides. ② The autoclave was preheated to 200 °C for 30 min and then the reaction progressed for 24 h.	Microrods	$\text{La}^{3+} + \text{Ln}^{3+} + \text{OH}^- \rightarrow \text{La(OH)}_3 : \text{Ln}^{3+}$
[20]	① Concentrated NH ₄ OH was dropped to La(NO ₃) ₃ ·6H ₂ O solution until pH at 10. ② Transfer into a Teflon-lined autoclave and heat by a 300 W microwave digestion at 150 °C for 1 h.	Nanowires	$\text{La}^{3+} + \text{OH}^- \rightarrow (\text{La(OH)}_4)^-$ $(\text{La(OH)}_4)^- + \text{NH}_4^+ \rightarrow \text{NH}_4\text{La(OH)}_4$ $\text{NH}_4\text{La(OH)}_4 \rightarrow \text{La(OH)}_3 + \text{NH}_4^+ + \text{OH}^-$

of the sample occurring in the conventional drying process [32]. The summary of preparation process of La(OH)₃ nanostructures by hydrothermal/solvothermal method is shown in Table 2.

3. Application of One-Dimensional La(OH)₃ Nanostructures

As the potential building blocks for future materials, 1D La(OH)₃ nanosystems exhibit unique physical properties due to their size and structure anisotropy. These properties have been exploited to the design and development of various electronic, fluorescent, and photocatalytic devices. In this context, 1D La(OH)₃ nanostructures represent an ideal channel for devices acting as capacitor and are suitable for biological labeling. In this section, applications based on photoluminescence, photocatalyst, and super capacitor will be presented.

3.1. Photoluminescence. To the best of our knowledge, La(OH)₃ nanostructures with higher crystallinity are important for phosphors. High crystallinity generally means less traps and stronger luminescence. In Jia's [17] experimental results, the luminescence properties of the as-obtained phosphors are dependent on their morphologies and sizes. The morphology and size of the lanthanide-base luminescent materials may affect the emission intensity as a result of the change in their specific surface area [33–35]. If the surface area is greatly reduced, which results in increased crystallite size, the phosphor with fewer defects would show great improvement in PL intensity [33–35]. Therefore, the nanowire phosphor has a higher PL intensity than nanoprism phosphor. As we know, the PL intensity of the phosphor is strongly influenced by the dopant concentration [36–38]. It has been proved that the Tb³⁺-doped La(OH)₃ samples

have the luminescence properties and exhibit strong green emission.

As known to all, lanthanum oxide is a promising host matrix for its good chemical durability, thermal stability, and low phonon energy, which result in high upconversion (UC) photoluminescence (PL) properties [39], while La₂O₃ doped by rare earth ions (RE) exhibits brighter luminescence than the purity of La₂O₃. The emission from the RE³⁺ dopants is mainly due to the electric and magnetic dipole optical transitions based on their unique intra-4f transitions, which are shielded by the outer 5s and 5p orbitals, consequently, leading to sharp emissions and narrow bands. Zhang et al. reported [20] that La₂O₃:Ln³⁺ microrods exhibit the characteristic emissions of Er³⁺, Tm³⁺, and Ho³⁺ and give rise to green, blue, and blackish green emission colors, respectively. In the codoped process, the emission intensities are governed by the concentration of Yb³⁺ ions. Of course, the unique fluorescent properties facilitate a promising candidate of this La₂O₃ based material in various color display fields on the basis of the high upconverting efficiency and high resistance against laser radiation damage.

3.2. Photocatalysis. Congo red (CR) is a well-known class of azo dyes that are of high toxicity and even carcinogenic to the animals and human. They are not readily degradable due to their complex aromatic structures [40]. However, photodegradation has been proved to be effective for this kind of pollution because of its strong destructive power to mineralize the pollutants into CO₂ and H₂O. The photocatalytic activity of La(OH)₃:Ln³⁺ nanorods used as the potential photocatalytic materials for photodegradation of Congo red in the aqueous solution has been reported [18]. The photocatalytic activity of semiconductor is based on the generation of electron (e⁻)-hole (h⁺) pair. The impurity level and the lattice defects are generated in the presence

of the singly ionized oxygen vacancy (V_0^+) defects in the as-synthesized $\text{La}(\text{OH})_3$; V_0^+ defect can work as electron donors to form charged oxygen vacancy (V_0^{++}) [41] and trap the photogenerated holes to reduce the surface recombination of electrons and holes [42]. Therefore, the more the singly ionized oxygen vacancy (V_0^+) defects, the higher the photocatalytic activity, while Ln doping is proposed to be located at substitutional positions instead of lanthanum site, so with increase in doping concentrations of Ln, the singly ionized oxygen vacancy (V_0^+) defect concentration increases; thus the corresponding photodegradation activity of $\text{La}(\text{OH})_3 : \text{Ln}^{3+}$ increases. Therefore, the enhanced photocatalytic activity may be ascribed to the lattice defects resulting from doping, which will accelerate the photogenerated electron-hole separation.

3.3. Super Capacitor. The material of $\text{La}(\text{OH})_3$ being dielectric may be used for fabrication of super capacitors. Generally speaking, conductivity maybe depends on three factors; the first term is dependent on frequency; the second term may be a result of autoionisation or polarization; the third which may be possible is that some of free La^{3+} ions were left entrapped inside the crystal structure which may generate defects in the $\text{La}(\text{OH})_3$ crystal. Kohli [16] has reported that capacitance values at lower frequency first decrease sharply and then slowly and become nearly constant. The capacitive behavior may be due to the space charge polarisation from inhomogeneous dielectric structure. Thus this type of electrical behavior may be useful for designing low loss super capacitors and sensors. Hu et al. [10] fabricated a pair of electrodes for connecting a single $\text{La}(\text{OH})_3$ nanobelt to characterize its electrical transport properties. The detectable conductive behavior of a single nanobelt promises the potential application of $\text{La}(\text{OH})_3$ nanobelts in capacitors and sensors.

4. Summary and Outlook

This paper provides an up-to-date review of the current achievements on 1D $\text{La}(\text{OH})_3$ nanomaterials, ranging from synthesis to applications. Synthesis of 1D structures has been well developed and an assortment of nanowires, nanobundles, nanobelts, and nanorods is successfully obtained. Such 1D $\text{La}(\text{OH})_3$ materials have provided a ground for fundamental studies as well as technological developments. The synthesis of 1D $\text{La}(\text{OH})_3$ nanostructure was influenced by many parameters such as temperature, time, PH value, alkaline source, surface energy, and surfactant. The length and diameter of the as-synthesized $\text{La}(\text{OH})_3$ nanowires were increased with the increasing reaction temperature and reaction time by hydrothermal method. The pH values of the initial solutions and the alkaline sources will influence the preferential growth orientations of nanocrystals, thus playing a crucial role in controlling the morphologies of the products. In general, the growth of nanostructure is closely related to two factors: the surface energy and growth kinetics, which determine the growth preferential and final structure, respectively. Surfactant can reduce the surface tension of the solution, which lower the energy needed to form a new

phase in reaction mixture. So surfactant-assisted synthesis is considered to be an effective methodology for shape-controlled synthesis in nanomaterials. The specific effects of different surfactants are different. Diethylenetriamine, acting not only as an alkaline source but also as a surfactant, induces the centripetal growth of $\text{La}(\text{OH})_3$ nanostructures. The cationic CTAB surfactant serves as a growth controller as well as agglomeration inhibitor by forming a covering film on the $\text{La}(\text{OH})_3$ rods. $\text{N}_2\text{H}_4 \cdot \text{H}_2\text{O}$ serving as crystal facet inhibitors lead to the formation of nanoprisms. The existing methods for fabricating $\text{La}(\text{OH})_3$ nanostructure usually need the assistance of surfactant; thus hunting for other methods to obtain the different morphology of $\text{La}(\text{OH})_3$ is necessary.

Furthermore, these fascinating researches mainly focus on the photoluminescence and photocatalyst area. The unique fluorescent properties of $\text{La}(\text{OH})_3$ make it a promising candidate in various color display fields on the basis of the high upconverting efficiency and high resistance against laser radiation damage. Moreover, $\text{La}(\text{OH})_3$ may find potential applications in many fields such as optoelectronic and nanoscale devices due to the unique luminescence properties and controllable morphology and size. The photocatalytic activity of semiconductor is based on the generation of electron-hole pairs, and $\text{La}(\text{OH})_3$ semiconductor can separate the electron-hole pairs. Therefore, $\text{La}(\text{OH})_3$ is a promising material for potential application in photodegradation pollutants. Besides, the as-synthesized $\text{La}(\text{OH})_3 : \text{Ln}^{3+}$ exhibit higher photodegradation activity compared with pure $\text{La}(\text{OH})_3$ due to the fact that doping can result in lattice defects. Nevertheless, there is much new science awaiting to elucidate, especially the mechanism of photocatalysis by $\text{La}(\text{OH})_3$ nanomaterials. In addition, except tuning the morphology of $\text{La}(\text{OH})_3$ nanostructure, technologies such as doping of nonmetal elements, surface modification, and formation of heterostructure can also be applied to improve the photocatalytic activity.

Conflict of Interests

The authors declare that there is no conflict of interests regarding the publication of this paper.

References

- [1] L.-X. Yang, Y. Liang, H. Chen, Y.-F. Meng, and W. Jiang, "Controlled synthesis of Mn_3O_4 and MnCO_3 in a solvothermal system," *Materials Research Bulletin*, vol. 44, no. 8, pp. 1753–1759, 2009.
- [2] Q. T. Li, J. S. Ni, Y. Q. Wu, Y. N. Du, W. Z. Ding, and S. Geng, "Synthesis and characterization of $\text{La}(\text{OH})_3$ nanopowders from hydrolysis of lanthanum carbide," *Journal of Rare Earths*, vol. 29, no. 5, pp. 416–419, 2011.
- [3] C. J. Murphy, T. K. Sau, A. M. Gole et al., "Anisotropic metal nanoparticles: synthesis, assembly, and optical applications," *The Journal of Physical Chemistry B*, vol. 109, no. 29, pp. 13857–13870, 2005.
- [4] J. W. Stouwdam, G. A. Hebbink, J. Huskens, and F. C. J. M. van Veggel, "Lanthanide-doped nanoparticles with excellent luminescent properties in organic media," *Chemistry of Materials*, vol. 15, no. 24, pp. 4604–4616, 2003.

- [5] L. F. Liang, H. F. Xu, Q. Su et al., "Hydrothermal synthesis of prismatic NaHoF_4 microtubes and NaSmF_4 nanotubes," *Inorganic Chemistry*, vol. 43, no. 5, pp. 1594–1596, 2004.
- [6] M. S. Palmer, M. Neurock, and M. M. Olken, "Periodic density functional theory study of methane activation over La_2O_3 : activity of O^{2-} , O^- , O_2^- , oxygen point defect, and Sr^{2+} -doped surface sites," *Journal of the American Chemical Society*, vol. 124, no. 28, pp. 8452–8461, 2002.
- [7] J. L. Zhuang, L. F. Liang, H. H. Y. Sung et al., "Controlled hydrothermal growth and up-conversion emission of NaLnF_4 ($\text{Ln} = \text{Y}, \text{Dy}, \text{Yb}$)," *Inorganic Chemistry*, vol. 46, no. 13, pp. 5404–5410, 2007.
- [8] X. Wang and Y. Li, "Synthesis and characterization of lanthanide hydroxide single-crystal nanowires," *Angewandte Chemie International Edition*, vol. 41, no. 24, pp. 4790–4793, 2002.
- [9] X. Wang, X. Sun, D. Yu, B. Zou, and Y. Li, "Rare earth compound nanotubes," *Advanced Materials*, vol. 15, no. 17, pp. 1442–1445, 2003.
- [10] C. G. Hu, H. Liu, W. T. Dong et al., " $\text{La}(\text{OH})_3$ and La_2O_3 nanobelts—synthesis and physical properties," *Advanced Materials*, vol. 19, no. 3, pp. 470–474, 2007.
- [11] I. Djerdj, G. Garnweitner, D. Sheng Su, and M. Niederberger, "Morphology-controlled nonaqueous synthesis of anisotropic lanthanum hydroxide nanoparticles," *Journal of Solid State Chemistry*, vol. 180, no. 7, pp. 2154–2165, 2007.
- [12] X. Wang and Y. D. Li, "Synthesis and characterization of lanthanide hydroxide single-crystal nanowires," *Angewandte Chemie*, vol. 41, no. 24, pp. 4790–4793, 2002.
- [13] Q. Mu, T. Chen, and Y. Wang, "Synthesis, characterization and photoluminescence of lanthanum hydroxide nanorods by a simple route at room temperature," *Nanotechnology*, vol. 20, no. 34, Article ID 345602, 2009.
- [14] S. G. Dixit, A. K. Vanjara, J. Nagarkar, M. Nikoorazm, and T. Desai, "Co-adsorption of quaternary ammonium compounds—nonionic surfactants on solid-liquid interface," *Colloids and Surfaces A*, vol. 205, no. 1-2, pp. 39–46, 2002.
- [15] S. C. Li, S. J. Hu, N. Du, J. N. Fan, L. J. Xu, and J. Xu, "Low-temperature chemical solution synthesis of dendrite-like $\text{La}(\text{OH})_3$ nanostructures and their thermal conversion to La_2O_3 nanostructures," *Rare Metals*, 2014.
- [16] P. S. Kohli, M. Kumar, K. K. Raina, and M. L. Singla, "Mechanism for the formation of low aspect ratio of $\text{La}(\text{OH})_3$ nanorods in aqueous solution: thermal and frequency dependent behaviour," *Journal of Materials Science: Materials in Electronics*, vol. 23, no. 12, pp. 2257–2263, 2012.
- [17] G. Jia, Y. Huang, Y. Song, M. Yang, L. Zhang, and H. You, "Controllable synthesis and luminescence properties of $\text{La}(\text{OH})_3$ and $\text{La}(\text{OH})_3:\text{ITb}^{3+}$ nanocrystals with multifiform morphologies," *European Journal of Inorganic Chemistry*, no. 25, pp. 3721–3726, 2009.
- [18] Y. Wang, S. Liu, Y. Cai et al., " $\text{La}(\text{OH})_3:\text{Ln}^{3+}$ ($\text{Ln} = \text{Sm}, \text{Er}, \text{Gd}, \text{Dy}$, and Eu) nanorods synthesized by a facile hydrothermal method and their enhanced photocatalytic degradation of Congo red in the aqueous solution," *Ceramics International*, vol. 40, no. 3, pp. 5091–5095, 2014.
- [19] O. Yayapao, S. Thongtem, A. Phuruangrat, and T. Thongtem, "A simple microwave-assisted hydrothermal synthesis of lanthanum hydroxide nanowires with a high aspect ratio," *Journal of Ceramic Processing Research*, vol. 13, no. 4, pp. 466–469, 2012.
- [20] X. Zhang, P. Yang, D. Wang et al., " $\text{La}(\text{OH})_3:\text{Ln}^{3+}$ and $\text{La}_2\text{O}_3:\text{Ln}^{3+}$ ($\text{Ln} = \text{Yb}/\text{Er}, \text{Yb}/\text{Tm}, \text{Yb}/\text{Ho}$) microrods: synthesis and up-conversion luminescence properties," *Crystal Growth and Design*, vol. 12, no. 1, pp. 306–312, 2012.
- [21] H. Liu, C. G. Hu, and Z. L. Wang, "Composite-hydroxide-mediated approach for the synthesis of nanostructures of complex functional-oxides," *Nano Letters*, vol. 6, no. 7, pp. 1535–1540, 2006.
- [22] C. G. Hu, H. Liu, C. S. Lao, L. Y. Zhang, D. Davidovic, and Z. L. Wang, "Size-manipulable synthesis of single-crystalline BaMnO_3 $\text{BaTi}_{1/2}\text{Mn}_{1/2}\text{O}_3$," *Journal of Physical Chemistry B*, vol. 110, no. 29, pp. 14050–14054, 2006.
- [23] J. Yang, C. K. Lin, Z. L. Wang, and J. Lin, " $\text{In}(\text{OH})_3$ and In_2O_3 nanorod bundles and spheres: microemulsion-mediated hydrothermal synthesis and luminescence properties," *Inorganic Chemistry*, vol. 45, no. 22, pp. 8973–8979, 2006.
- [24] S. Möhmel, I. Kurzawski, D. Uecker, D. Müller, and W. Geßner, "The influence of a hydrothermal treatment using microwave heating on the crystallinity of layered double hydroxides," *Crystal Research and Technology*, vol. 37, no. 4, pp. 359–369, 2002.
- [25] X. Y. Ma, H. Zhang, Y. J. Ji, J. Xu, and D. Yang, "Synthesis of ultrafine lanthanum hydroxide nanorods by a simple hydrothermal process," *Materials Letters*, vol. 58, no. 7-8, pp. 1180–1182, 2004.
- [26] F. V. Motta, R. C. Lima, A. P. A. Marques et al., "Indium hydroxide nanocubes and microcubes obtained by microwave-assisted hydrothermal method," *Journal of Alloys and Compounds*, vol. 497, no. 1-2, pp. L25–L28, 2010.
- [27] G. Glaspell, L. Fuoco, and M. S. El-Shall, "Microwave synthesis of supported Au and Pd nanoparticle catalysts for CO oxidation," *Journal of Physical Chemistry B*, vol. 109, no. 37, pp. 17350–17355, 2005.
- [28] M. Mazloumi, S. Zanganeh, A. Kajbafvala, M. R. Shayegh, and S. K. Sadrnezhad, "Formation of Lanthanum hydroxide nanostructures: effect of NaOH and KOH solvents," *International Journal of Engineering, Transactions B: Applications*, vol. 21, no. 2, pp. 169–176, 2008.
- [29] K. Tang, Y. Qian, J. Zeng, and X. Yang, "Solvothermal route to semiconductor nanowires," *Advanced Materials*, vol. 15, no. 5, pp. 448–450, 2003.
- [30] K. Byrappa and M. Yoshimura, "Hydrothermal technology for nanotechnology," in *Handbook of Hydrothermal Technology*, pp. 615–762, 2013.
- [31] B. Tang, J. C. Ge, C. J. Wu et al., "Sol-solvothermal synthesis and microwave evolution of $\text{La}(\text{OH})_3$ nanorods to La_2O_3 nanorods," *Nanotechnology*, vol. 15, no. 9, pp. 1273–1276, 2004.
- [32] K. J. Rao, B. Vaidhyanathan, M. Ganguli, and P. A. Ramakrishnan, "Synthesis of inorganic solids using microwaves," *Chemistry of Materials*, vol. 11, no. 4, pp. 882–895, 1999.
- [33] J. Yang, C. Li, Z. Cheng et al., "Size-tailored synthesis and luminescent properties of one-dimensional $\text{Gd}_2\text{O}_3:\text{Eu}^{3+}$ nanorods and microrods," *Journal of Physical Chemistry C*, vol. 111, no. 49, pp. 18148–18154, 2007.
- [34] J. Yang, X. M. Liu, C. X. Li, Z. W. Quan, D. Y. Kong, and J. Lin, "Hydrothermal synthesis of $\text{SrCO}_3:\text{Eu}^{3+}/\text{Tb}^{3+}$ microneedles and their luminescence properties," *Journal of Crystal Growth*, vol. 303, no. 2, pp. 480–486, 2007.
- [35] J. Wan, Z. Wang, X. Chen, L. Mu, and Y. Qian, "Shape-tailored photoluminescent intensity of red phosphor $\text{Y}_2\text{O}_3:\text{Eu}^{3+}$," *Journal of Crystal Growth*, vol. 284, no. 3-4, pp. 538–543, 2005.
- [36] M. Yu, J. Lin, Z. Wang et al., "Fabrication, patterning, and optical properties of nanocrystalline $\text{YVO}_4:\text{A}$ ($\text{A} = \text{Eu}^{3+}, \text{Dy}^{3+}, \text{Sm}^{3+}, \text{Er}^{3+}$) phosphor films via sol-gel soft lithography," *Chemistry of Materials*, vol. 14, no. 5, pp. 2224–2231, 2002.
- [37] K. Kim, Y. Kim, H. Chun, T. Cho, J. Jung, and J. Kang, "Structural and optical properties of $\text{BaMgAl}_{10}\text{O}_{17}:\text{Eu}^{2+}$ phosphor," *Chemistry of Materials*, vol. 14, no. 12, pp. 5045–5052, 2002.

- [38] K. Y. Jung, H. W. Lee, and H. Jung, "Luminescent properties of (Sr, Zn)Al₂O₄:Eu²⁺, B³⁺ particles as a potential green phosphor for UV LEDs," *Chemistry of Materials*, vol. 18, no. 9, pp. 2249–2255, 2006.
- [39] H. Q. Liu, L. L. Ying, and S. G. Chen, "Effect of Yb³⁺ concentration on the upconversion of Er³⁺ ion doped La₂O₃ nanocrystals under 980 nm excitation," *Materials Letters*, vol. 61, no. 17, pp. 3629–3631, 2007.
- [40] Z. J. Yang, J. J. Wei, H. X. Yang, L. Liu, H. Liang, and Y. Z. Yang, "Mesoporous CeO₂ hollow spheres prepared by ostwald ripening and their environmental applications," *European Journal of Inorganic Chemistry*, no. 21, pp. 3354–3359, 2010.
- [41] S. Y. Liu, Y. Cai, X. Y. Cai et al., "Catalyzed degradation Congo red in the aqueous solution by Ln(OH)₃ (Ln1/4Nd, Sm, Eu, Gd, Tb, and Dy) nanorods," *Applied Catalysis A*, vol. 453, pp. 45–53, 2013.
- [42] Y. Hu and H.-J. Chen, "Origin of green luminescence of ZnO powders reacted with carbon black," *Journal of Applied Physics*, vol. 101, no. 12, pp. 124902–124905, 2007.



Hindawi

Submit your manuscripts at
<http://www.hindawi.com>

